Malaysian Journal of Mathematical Sciences 13(3): 397–418 (2019)

MALAYSIAN JOURNAL OF MATHEMATICAL SCIENCES

Journal homepage: http://einspem.upm.edu.my/journal

Magnetoconvection on the Double–Diffusive Nanofluids Layer Subjected to Internal Heat Generation in the Presence of Soret and Dufour Effects

Khalid, I. K.[1], Mokhtar, N. F. M. *[1,2], Siri, Z. [3], Ibrahim, Z. B. [1,2], and Abd Gani, S. S. [4]

[1]*Institute for Mathematical Research, Universiti Putra Malaysia, Malaysia*
[2]*Department of Mathematics, Faculty of Science, Universiti Putra Malaysia, Malaysia*
[3]*Institute for Mathematical Sciences, Faculty of Science, Universiti Malaya, Malaysia*
[4]*Department of Agriculture Technology, Faculty of Agriculture, Universiti Putra Malaysia, Malaysia*

E-mail: norfadzillah.mokhtar@gmail.com
* *Corresponding author*

Received: 27 December 2017
Accepted: 16 March 2019

ABSTRACT

Combination of magnetic field and internal heat generation effects on double-diffusive convection in nanofluids layer is applied in the existence of Soret and Dufour effects. The model employed for the nanofluids associates with the Brownian motion and thermophoresis. Linear stability theory upon normal mode technique is used and the eigenvalue solution is obtained by using the Galerkin technique. On the stationary convection,

it is observed that the application of magnetic field stabilizes the system while internal heat generation destabilizes the system. The analysis also reveals that it is possible to delay the onset of convection through nanofluids parameters in the system.

Keywords: Magnetic field, internal heat generation, nanofluids, Soret and Dufour.

1. Introduction

Rapid development in these new engineered fluids called nanofluids have uncovered an advance approach in the heat transfer mechanism due to its stability in the research area that has attracted many researchers attention. The earliest phenomenon observations of thermal conductivity enhancement in nanofluids were reported by Masuda et al. (1993) and the term nanofluids has been proposed by Choi (1995), a colloidal mixture of base fluids (nanoparticles fluids suspensions) with a nanoparticles (1-100 nm) at the Argonne National Laboratory, U.S.A. Buongiorno (2006) investigated nanofluids, the engineered colloids that made of base fluids and nano-sized particles. Seven slip mechanisms have been considered that can produce a relative velocity between the nanoparticles and the base fluids such as gravity, Brownian motion, inertia, thermophoresis, Magnus effect, diffusiophoresis, and fluid drainage. They summarized and only included the Brownian motion and thermophoresis slip mechanisms in nanofluids model. Tzou (2008a) studied the case of stress free boundaries, meanwhile, Tzou (2008b) investigated the combination of one free and one rigid boundary, and the case of two rigid boundaries was briefly discussed.

In these papers, the problems considered by Tzou (2008a,b) are revisited with the goal of clarifying the physical mechanism involved in instability development and extending the results to the mode of oscillatory thermal instability. Linear stability analysis on the onset of convection in nanofluids layer upon normal mode technique of finite depth was investigated by Nield and Kuznetsov (2010) by using Buongiorno's model of nanofluids. For completeness, it is to mention that a substantially different treatment of Bénard problem for nanofluids is given by Kim et al. (2004). These authors simply modified three quantities namely the thermal expansion coefficients, thermal diffusivity and kinematic viscosity that appear in the definition of Rayleigh number. Yadav et al. (2011) studied the Rayleigh-Bénard convective instability in nanofluids for alumina-water and copper-water. Meanwhile, Haddad et al. (2012) studied the onset of natural convection heat transfer and fluids flow of copper oxide-water nanofluids using the Rayleigh-Bénard problem. Thermal instability of rotating nanofluids

layer has been revised and analysed by Yadav et al. (2016).

The phenomena of double-diffusive convection is crucial in many practical and theoretical studies for both non-Newtonian and Newtonian fluids. Caldwell (1970) experimentally investigated the Rayleigh-Bénard experiment using a salt solution. Hurle and Jakeman (1971) used a water–methanol mixture on convective heat transfer induced by Soret in theoretical and experimental investigation. The linear stability of experimental Soret convection in a water–ethanol mixture under various boundary conditions has been investigated by Knobloch and Moore (1988). The thermocapillary instability in binary fluids on the onset of convection by considering the Soret effect with other physical influences has been studied by Bergeon et al. (1998), Saravanan and Sivakumar (2009), Slavtchev et al. (1999). In 2011, Nield and Kuznetsov (2011) studied the linear instability theory on the onset of double-diffusive convection in a horizontal layer of nanofluids. Kuznetsov and Nield (2010), Yadav et al. (2012a,b), and Agarwal et al. (2012) investigated double-diffusive convection in a porous medium permeated by nanofluids layer. The following authors, Akbar et al. (2016), Chand and Rana (2015), added other effects to the system of double-diffusive convection in nanofluids layer. Meanwhile, Khalid et al. (2017), Mokhtar et al. (2017) examined the system of double-diffusive convection with the effects of feedback control as well as rotation.

The study on the onset of convective instability with the effects of magnetic field has attracted many researchers attention. Convection in horizontal layer of electrically conducting fluids subjected to gravity and magnetic field is called magnetoconvection. The cause of magnetoconvection is the combined effects of buoyancy force and Lorentz force in the presence of a magnetic field which has many important applications in physics and engineering. Chandrasekhar (1961) showed the critical value of Rayleigh number can be increased through the use of the effect of magnetic field and stabilized the system. The thermal instability under the influences of increasing the value of magnetic field is possible to delay the onset of convection Rama Rao (1980). Several authors claimed that the effect of increasing the intensity of the magnetic field makes the system to become more stable Maekawa and Tanasawa (1988), Rudraiah et al. (1984), Wilson (1994). Yadav et al. (2013) and Gupta et al. (2013) investigated the effect of the stabilizing magnetic field in nanofluids layer.

Thermal instability induced by internal heat source appears in numerous physical problems and has been extensively investigated by many researchers. The destabilizing effect of internal heat source has been investigated by Char and Chiang (1994). The effect of increasing the internal heat generation on Marangoni convection in a fluid saturated porous medium and superposed lay-

ers of fluid-porous is found to advance the onset of convection Mokhtar et al. (2009, 2010, 2011). These authors have added other effects with the effect of internal heat source in their research investigation Bhadauria et al. (2011), Capone et al. (2011), Friedrich and Rudraiah (1984). The application of the combination effects of magnetic field and internal heat generation to the system give evidences that magnetic field is always to stabilize the system while internal heat generation is to destabilize the system Khalid et al. (2013), Yadav et al. (2015).

This literature survey indicates that there is no other study has investigated the combination effects of magnetic field with internal heat generation in the presence of Dufour and Soret effects on the onset of double-diffusive convection in nanofluids layer is considered. Three types of bounding surfaces (lower boundary-upper boundary) are considered in this investigation: free-free, rigid-free and rigid-rigid. A linear stability analysis is performed upon normal mode technique, and the eigenvalue is obtained by employing the Galerkin technique. Numerical computations of the various relevant parameters are computed by Maple software and presented graphically.

2. Mathematical Formulation

The Cartesian coordinates (x, y, z) are used, where the z-axis points vertically upward. Consider a horizontal nanofluids layer of thickness L confined between the planes $z^* \in [0, L]$, subjected to uniform vertical magnetic field, $\boldsymbol{h}= (0, 0, h_0^*)$, internal heat generation G_0^* and double-diffusive coefficients as shown in Figure 1 are examined. The temperature, solute concentration, and volumetric fraction of nanoparticles at the lower and upper walls are denoted by T_l^*, C_l^*, ϕ_l^* at $z = 0$ and T_u^*, C_u^*, and ϕ_u^* at $z = L$, respectively. The applicable governing equations to describe the Boussinesq flow under this figure and model below.

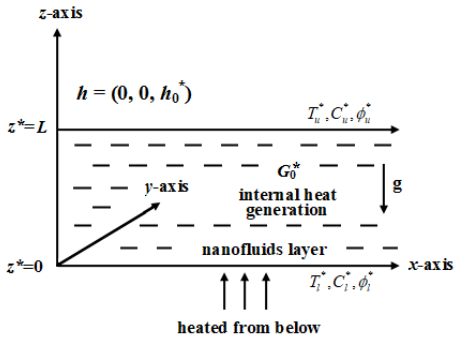

Figure 1: Physical configuration.

The model are

$$\nabla^* \cdot \boldsymbol{V}^* = 0, \tag{1}$$

$$\rho_l \left[\frac{\partial \boldsymbol{V}^*}{\partial t^*} + (\boldsymbol{V}^* \cdot \nabla^*)\boldsymbol{V}^*\right] = -\nabla^* p^* + \mu \nabla^{*2}\boldsymbol{V}^* + \frac{\mu_e}{4\pi}(\boldsymbol{h}^* \cdot \nabla^*)\boldsymbol{h}^* + \mathbf{g}\left[\phi^*\rho_p + (1-\phi^*)\rho_l\left[1 - \alpha_T(T^* - T_l^*) - \alpha_C(C^* - C_l^*)\right]\right], \tag{2}$$

$$\rho c \left[\frac{\partial T^*}{\partial t^*} + (\boldsymbol{V}^* \cdot \nabla^*)T^*\right] = \kappa \nabla^{*2} T^* + \rho c \left[D_{TC}\nabla^{*2} C^*\right] + G_0^* + \rho_p c_p \left[D_B \nabla^* \phi^* \cdot \nabla^* T^* + (\tfrac{D_T}{T_u^*})\nabla^* T^* \cdot \nabla^* T^*\right], \tag{3}$$

$$\left[\frac{\partial C^*}{\partial t^*} + (\boldsymbol{V}^* \cdot \nabla^*)C^*\right] = D_{CT}\nabla^{*2} T^* + D_S \nabla^{*2} C^*, \tag{4}$$

$$\left[\frac{\partial \phi^*}{\partial t^*} + (\boldsymbol{V}^* \cdot \nabla^*)\phi^*\right] = \frac{D_T}{T_u^*}\nabla^{*2} T^* + D_B \nabla^{*2}\phi^*, \tag{5}$$

$$\left[\frac{\partial \boldsymbol{h}^*}{\partial t^*} + (\boldsymbol{V}^* \cdot \nabla^*)\boldsymbol{h}^*\right] = (\boldsymbol{h}^* \cdot \nabla^*)\boldsymbol{V}^* + \eta \nabla^{*2}\boldsymbol{h}^*, \tag{6}$$

$$\nabla^* \cdot \boldsymbol{h}^* = 0, \tag{7}$$

where $\boldsymbol{V}^* = (u, v, w)$ as velocity, ρ_l as nanofluids density at the reference temperature T_l^*, t^* as time, p^* as pressure, μ as viscosity, $\mu_e = \phi^*\mu_{ep} + (1-\phi^*)\mu_{ef}$ as magnetic permeability, $\boldsymbol{h}^* = (h_x, h_y, h_z)$ as magnetic field, $\mathbf{g}$ as gravitational force, ϕ^* as volumetric fraction of nanoparticles, ρ_p as nanoparticles mass density, α_T as thermal volumetric coefficient, T^* as temperature, α_C as solutal volumetric coefficient, C^* as solute concentration, ρ as density, c as specific heat, κ as nanofluid's thermal conductivity, G_0^* as uniform internal heat generation, D_{TC} as Dufour diffusivity, c_p as specific heat of nanoparticles, D_B as Brownian diffusion coefficient, D_T as thermophoretic diffusion coefficient, D_S as solutal diffusivity, D_{CT} as Soret diffusivity and $\eta = \phi^*\eta_p + (1-\phi^*)\eta_f$ as

electrical resistivity and the subscript p and f denotes as particles and fluid state.

In the steady state, the upper surface of the nanofluids layer is flat and stationary. Following Char and Chiang (1994), the pressure and temperature fields are

$$p^*(z) = p_l^* - \rho_l \left[1 + \frac{\alpha z^* \Delta T^*}{2L} - \frac{\alpha L \Delta T^*}{2L}\right] \mathbf{g}(z^* - L), \tag{8}$$

$$T^*(z) = T_l^* - \frac{G_0^*}{2\kappa} z^{*2} + \frac{G_0^* L}{2\kappa} z^* - \frac{\Delta T^*}{L} z^*, \tag{9}$$

where p_l^* as reference pressure, and ΔT^* as temperature difference across the fluid layer. Then, Equations (1)-(7) are nondimensionalized using the following definitions:

$$(x, y, z) = \frac{x^*, y^*, z^*}{L}, p = L^2 \frac{p^*}{\mu \alpha_f}, t = \alpha_f \frac{t^*}{L^2}, T = \frac{T^* - T_l^*}{\Delta T^*}, \phi = \frac{\phi^* - \phi_l^*}{\phi_u^* - \phi_l^*},$$
$$(u, v, w) = L \frac{u^*, v^*, w^*}{\alpha_f}, C = \frac{C^* - C_l^*}{\Delta C^*}, (h_x, h_y, h_z) = \frac{(h_x^*, h_y^*, h_z^*)}{h_0^*}, \tag{10}$$

where $\alpha_f = \frac{\kappa}{\rho c}$ as thermal diffusivity.

Substituting Equation (10) into Equations (1)–(7), the following nondimensional variables are obtained:

$$\nabla \cdot \boldsymbol{V} = 0, \tag{11}$$

$$\frac{1}{Pr}\left[\frac{\partial \boldsymbol{V}}{\partial t} + \boldsymbol{V} \cdot \nabla \boldsymbol{V}\right] = -\nabla p + \nabla^2 \boldsymbol{V} - Rm\hat{\boldsymbol{e}}_{\boldsymbol{z}} + RaT\hat{\boldsymbol{e}}_{\boldsymbol{z}} + \frac{Rs}{Le} C\hat{\boldsymbol{e}}_{\boldsymbol{z}} - Rn\phi\hat{\boldsymbol{e}}_{\boldsymbol{z}} + H\frac{Pr}{Pm}(\boldsymbol{h} \cdot \nabla)\boldsymbol{h}, \tag{12}$$

$$\left[\frac{\partial T}{\partial t} + \boldsymbol{V} \cdot \nabla T\right] = \nabla^2 T + \frac{N_B}{Ln} \nabla\phi \cdot \nabla T + \frac{N_A N_B}{Ln} \nabla T \cdot \nabla T + Df \nabla^2 C + [Q(1 - 2z) - 1]\, w, \tag{13}$$

$$\left[\frac{\partial C}{\partial t} + \boldsymbol{V} \cdot \nabla C\right] = \frac{1}{Le} \nabla^2 C + Sr \nabla^2 T, \tag{14}$$

$$\left[\frac{\partial \phi}{\partial t} + \boldsymbol{V} \cdot \nabla \phi\right] = \frac{1}{Ln} \nabla^2 \phi + \frac{N_A}{Ln} \nabla^2 T, \tag{15}$$

$$\left[\frac{\partial \boldsymbol{h}}{\partial t} + \boldsymbol{V} \cdot \nabla \boldsymbol{h}\right] = (\boldsymbol{h} \cdot \nabla)\boldsymbol{V} + \frac{Pm}{Pr} \nabla^2 \boldsymbol{h}, \tag{16}$$

$$\nabla \cdot \boldsymbol{h} = 0, \tag{17}$$

where $Pr = \frac{\mu}{\rho \alpha_f}$ as Prandtl number, $\hat{\boldsymbol{e}}_{\boldsymbol{z}} = (0, 0, 1)$ as unit vector in the z direction, $Rm = \frac{[\rho_p \phi_l^* + \rho(1 - \phi_l^*)] g L^3}{\mu \alpha_f}$ as basic-density Rayleigh number, $Ra = \frac{\rho g \alpha_T L^3 \Delta T^*}{\mu \alpha_f}$ as thermal Rayleigh number, $Rs = \frac{\rho g \alpha_C L^3 \Delta C^*}{\mu D_s}$ as solutal Rayleigh

number, $Le = \frac{\alpha_f}{D_s}$ as Lewis number, $Rn = \frac{(\rho_p - \rho)(\phi_u^* - \phi_l^*)gL^3}{\mu\alpha_f}$ as nanoparticle concentration Rayleigh number, $H = d^2 \frac{\mu_{ef} h_0^{*2}}{4\pi\rho\eta_f\mu}$ as Chandrasekhar number, $Pm = \frac{\mu}{\alpha_f \eta}$ as magnetic Prandtl number, $N_B = \frac{(\rho c)_p}{(\rho c)_f}(\phi_u^* - \phi_l^*)$ as modified particle-density increment, $Ln = \frac{\alpha_f}{D_B}$ as nanofluid Lewis number, $N_A = \frac{D_T \Delta T^*}{D_B T_u^* (\phi_u^* - \phi_l^*)}$ as modified density ratio, $Df = \frac{D_{TC}\Delta C^*}{\alpha_f \Delta T^*}$ as Dufour parameter, $Q = \frac{G_0^* L^2}{2\kappa \Delta T^*}$ as internal heat generation and $Sr = \frac{D_{CT}\Delta T^*}{\alpha_f \Delta C^*}$ as Soret parameter.

The upper boundary is assumed to be nondeformable and the basic state of the nanofluids is quiescent (at rest) with temperature, solute concentration, and volumetric fraction of nanoparticles varying only in the z direction, that is, a basic state solution of the form

$$(u, v, w) = (0, 0, 0), p = p_b(z), T = T_b(z), C = C_b(z), \phi = \phi_b(z), \boldsymbol{h} = \hat{\boldsymbol{e}}_z. \quad (18)$$

Let the basic state be disturbed by an infinitesimal thermal perturbation. We now superimpose perturbations on the basic solution. We write

$$\begin{gathered} \boldsymbol{V} = \boldsymbol{V'}, p = p_b(z) + p', T = T_b(z) + T', C = C_b(z) + C', \\ \phi = \phi_b(z) + \phi', \boldsymbol{h} = \hat{\boldsymbol{e}}_z + \boldsymbol{h'}. \end{gathered} \quad (19)$$

We substitute Equation (19) into Equations (11)–(17) and linearise them by neglecting the products of primed quantities. The following equations are obtained when Equation (18) is used:

$$\nabla \cdot \boldsymbol{V}' = 0, \quad (20)$$

$$\begin{aligned} \frac{1}{Pr}\frac{\partial \boldsymbol{V}'}{\partial t} = -\nabla p' + \nabla^2 \boldsymbol{V}' + RaT'\hat{\boldsymbol{e}}_{\boldsymbol{z}} + \frac{Rs}{Le}C'\hat{\boldsymbol{e}}_{\boldsymbol{z}} - Rn\phi'\hat{\boldsymbol{e}}_{\boldsymbol{z}} + \\ H\frac{Pr}{Pm}\left(\frac{\partial \boldsymbol{h'}}{\partial z}\right), \end{aligned} \quad (21)$$

$$\begin{aligned} \frac{\partial T'}{\partial t} - [Q(1-2z) - 1]\, w' = \nabla^2 T' + \frac{N_B}{Ln}\left[\frac{\partial T'}{\partial z} - \frac{\partial \phi'}{\partial z}\right] - \frac{2N_A N_B}{Ln}\frac{\partial T'}{\partial z} + \\ Df\nabla^2 C', \end{aligned} \quad (22)$$

$$\left[\frac{\partial C'}{\partial t} - w'\right] = \frac{1}{Le}\nabla^2 C' + Sr\nabla^2 T', \quad (23)$$

$$\left[\frac{\partial \phi'}{\partial t} + w'\right] = \frac{1}{Ln}\nabla^2 \phi' + \frac{N_A}{Ln}\nabla^2 T', \quad (24)$$

$$\frac{\partial \boldsymbol{h'}}{\partial t} = \frac{\partial w'}{\partial z}\hat{\boldsymbol{e}}_{\boldsymbol{z}} + \frac{Pm}{Pr}\nabla^2 \boldsymbol{h'}, \quad (25)$$

$$\nabla \cdot \boldsymbol{h'} = 0, \quad (26)$$

Applying $\hat{\boldsymbol{e}}_{\boldsymbol{z}}\cdot$ curl curl to Equation (21) and using the identity curl curl = grad div - ∇^2, together with Equation (20) and Equation (26), then, combined the resulting Equation (21) with Equation (25), thus, we obtain

$$\left[\nabla^4 - \frac{1}{Pr}\frac{\partial}{\partial t}\nabla^2\right] w' + \frac{Rs}{Le}\nabla_P^2 C' - Rn\nabla_P^2\phi' + Ra\nabla_P^2 T' - H\frac{Pr}{Pm}\frac{\partial}{\partial z}\left(\frac{\partial w'}{\partial z} - \frac{\partial h_z'}{\partial z}\right) = 0, \tag{27}$$

where ∇_P^2 is the horizontal two–dimensional Laplacian operator.

The proposed normal mode representation is as follows:

$$(w', T', C', \phi') = [W(z), \Theta(z), \eta(z), \phi(z)]\, e^{[i(a_x x + a_y y) + \sigma t]}, \tag{28}$$

where (a_x, a_y) is the wavevector in the (x, y) plane, $a^2 = a_x^2 + a_y^2$ is the square of the wavenumber, and σ is the growth parameter.

Substituting Equation (28) into Equations (22)–(24) and (27) neglecting the terms of the second and higher orders in the perturbations, we obtain

$$\left(D^2 - a^2\right)^2 W - a^2 Ra\Theta - a^2\frac{Rs}{Le}\eta + a^2 Rn\phi W - HD^2 W = 0, \tag{29}$$

$$[1 - Q(1-2z)]W + \left[D^2 - a^2 + \frac{N_B}{Ln}D - 2\frac{N_A N_B}{Ln}D\right]\Theta - \frac{N_B}{Ln}D\phi + Df(D^2 - a^2)\eta = 0, \tag{30}$$

$$W + Sr(D^2 - a^2)\Theta + \frac{1}{Le}(D^2 - a^2)\eta = 0, \tag{31}$$

$$W - \frac{N_A}{Ln}(D^2 - a^2)\Theta - \frac{1}{Ln}(D^2 - a^2)\phi = 0, \tag{32}$$

where $D = \frac{d}{dz}$ and $a = \sqrt{a_x^2 + a_y^2}$ is the wavenumber.

Equations (29)–(32) are solved subject to the appropriate boundary conditions below.

For the lower free and upper free boundaries

$$W = D^2 W = \Theta = \phi = \eta = 0 \text{ at } z = 0,$$
$$W = D^2 W = D\Theta = \phi = \eta = 0 \text{ at } z = 1. \tag{33}$$

For the lower rigid and upper free boundaries

$$W = DW = \Theta = \phi = \eta = 0 \text{ at } z = 0,$$
$$W = D^2 W = D\Theta = \phi = \eta = 0 \text{ at } z = 1. \tag{34}$$

For the lower rigid and upper rigid boundaries

$$W = DW = \Theta = \phi = \eta = 0 \text{ at } z = 0,$$
$$W = DW = D\Theta = \phi = \eta = 0 \text{ at } z = 1. \tag{35}$$

The Galerkin–type weighted residuals method is applied to find an approximate solution to the system. The variables are written in a series of basis functions as

$$W = \sum_{i=1}^{n} A_i W_i, \Theta = \sum_{i=1}^{n} B_i \Theta_i, \eta = \sum_{i=1}^{n} C_i \eta_i, \phi = \sum_{i=1}^{n} D_i \phi_i, \tag{36}$$

where A_i, B_i, C_i, and D_i are constants, and the base functions—W_i, Θ_i, η_i and ϕ_i, and $i = 1, 2, 3...$—are chosen respective to the lower-upper boundary conditions of free-free, rigid-free, and rigid-rigid:

$$W = \eta = \phi = sin(z\pi), \Theta = z(2 - z), \tag{37}$$
$$W = z^2(1 - z)(3 - 2z), \Theta = z(2 - z), \eta = \phi = z(1 - z), \tag{38}$$
$$W = z^2(1 - z)^2, \Theta = z(2 - z), \eta = \phi = z(1 - z). \tag{39}$$

We substitute Equation (36) into Equations (29)-(32) and make the expressions on the left-hand sides of those equations (the residuals) orthogonal to the trial functions, thereby obtaining a system of $4N$ linear algebraic equations with $4N$ unknowns. The elimination of the determinant of the coefficients produces the eigenvalue equation for the system. One can regard Ra as the eigenvalue, and thus Ra is found in terms of the other parameters.

We perform integration by parts with respect to z for $z \in [0, 1]$. By using the boundary conditions in Equations (37)–(39), we obtain a system of linear homogeneous algebraic equations:

$$a_{ji} W_i + b_{ji} \Theta_i + c_{ji} \eta_i + d_{ji} \phi_i = 0, \tag{40}$$
$$f_{ji} W_i + g_{ji} \Theta_i + h_{ji} \eta_i + i_{ji} \phi_i = 0, \tag{41}$$
$$k_{ji} W_i + l_{ji} \Theta_i + m_{ji} \eta_i + n_{ji} \phi_i = 0, \tag{42}$$
$$p_{ji} W_i + q_{ji} \Theta_i + r_{ji} \eta_i + s_{ji} \phi_i = 0. \tag{43}$$

The above set of homogeneous algebraic equations can have a non–trivial solution if and only if

$$\begin{vmatrix} a_{ji} & b_{ji} & c_{ji} & d_{ji} \\ f_{ji} & g_{ji} & h_{ji} & i_{ji} \\ k_{ji} & l_{ji} & m_{ji} & n_{ji} \\ p_{ji} & q_{ji} & r_{ji} & s_{ji} \end{vmatrix} = 0. \tag{44}$$

The eigenvalue has to be extracted using the characteristics of Equation (44).

3. Results and Discussions

The onset of magnetoconvection in rotating horizontal layer of nanofluids with internal heat generation subjected to double–diffusive coefficients is developed. The model used for nanofluids includes the combination effects of Brownian motion and thermophoresis. Linear stability analysis is employed, and the resulting eigenvalue, that is, the thermal Rayleigh number Ra parameter used to show the strength of buoyancy force, is extracted using the Galerkin technique. Three types of lower–upper boundary conditions are considered for stationary convection: free–free, rigid–free, and rigid–rigid, respectively. The bounded model of horizontal layer of nanofluids identifies that both thermophoresis and Brownian motion mechanisms enhanced the onset of convection. The obtained results are presented graphically and are illustrated in Figures 2-14.

To validate the accuracy of our numerical results, test computations are performed for comparison with the results of Nield and Kuznetsov (2011) regarding the omission of the magnetic field H, internal heat generation Q, and other relevant parameters. We find that the obtained critical Rayleigh number Ra_c is equivalent to that in the earlier work Nield and Kuznetsov (2011), where the values of Ra_c for lower–upper boundary conditions of free-free, rigid-free, and rigid-rigid are 657.5, 1140, and 1750, respectively.

Figure 2 shows a visual representation of thermal Rayleigh number Ra against wavenumber a for various values of the magnetic field, $H = 10$, 15, and 20 under various horizontal boundary conditions. Based on the observation, the greater strength of magnetic field H increases the values of Ra. This phenomenon causes a reduction in the rate Rayleigh-Bénard convection and stabilizes the system. Meanwhile, Figure 3 shows the marginal stability curves of different values of the internal heat generation, $Q = 3$, 6, and 9 under various horizontal boundary conditions. The induced internal heat generation decreases Ra, thus accelerating the onset of Rayleigh-Bénard convection. Therefore, enhanced heat transfer to the system occurs more rapidly with the induced internal heat generation as its effect increases the rate of disturbances in the nanofluids layer and introduces chaos in the entire system.

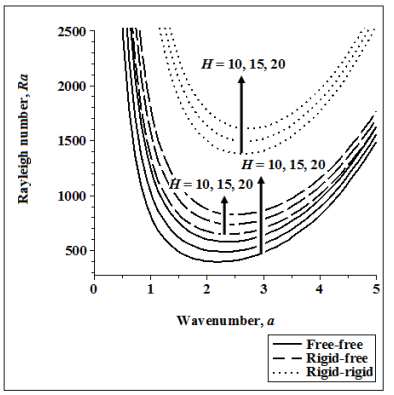

Figure 2: Ra against a for selected values of H.

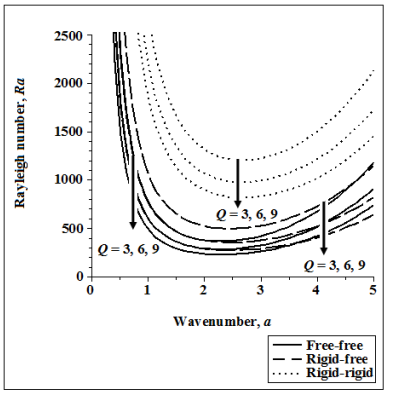

Figure 3: Ra against a for selected values of Q.

Figure 4 depicts the marginal stability curves for the three types of boundary conditions and various thermo-solutal Rayleigh numbers, $Rs = 100, 200$, and 300, in double-diffusive nanofluids layer. Parameter Rs is defined as the solute concentration within the fluid layer and the increase values of Rs have a positive significant impact on the stability of the nanofluids layer, where it is found that Ra increases monotonically. This result reveals that heat transfer within the nanofluids layer can be delayed when the amount of solute concentration is greater than that of the solvent, leading to a decrease in the overall temperature within the system. Therefore, Rs helps to stabilize the system.

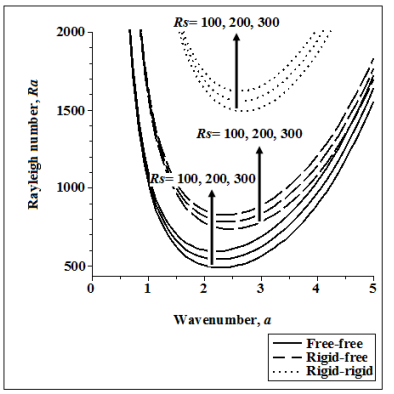

Figure 4: Ra against a for selected values of Rs.

Figure 5 shows the thermal Rayleigh number Ra against wavenumber a for various positive values of the nanoparticles concentration Rayleigh number, $Rn = 1, 2$, and 3, under various boundary conditions. Based on the definition of $Rn = \frac{(\rho_p - \rho)(\phi_u^* - \phi_l^*)gL^3}{\mu\alpha_f}$, it is found that the increase in Rn will increase the volumetric fraction of nanoparticles, ϕ^*, this results in the combination of Brownian motion and thermophoresis diffusion within the nanofluids layer that enhanced the thermal instability and destabilizes the system.

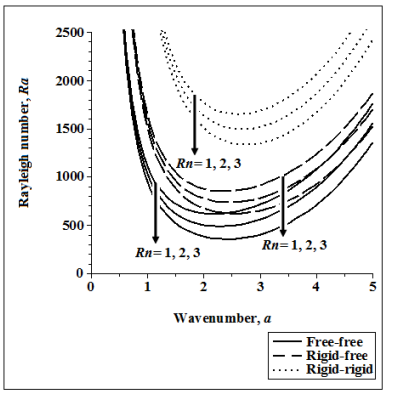

Figure 5: Ra against a for selected values of Rn.

Figure 6 corresponds to the Rayleigh number Ra for $N_A = 1, 5$, and 10 respectively. From the figure, the values of Rayleigh number Ra decreases only slightly with increasing of the modified diffusivity ratio N_A under three

lower–upper boundary conditions.

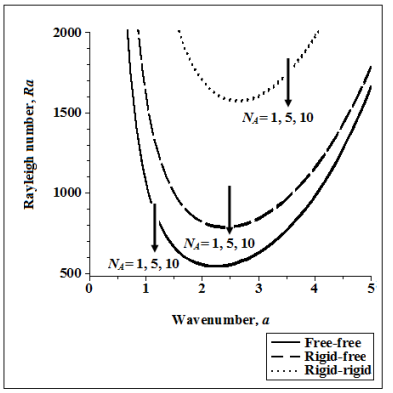

Figure 6: Ra against a for selected values of N_A.

Using the directly relationship between the parameter N_A and the thermophoretic diffusion coefficient D_T from $N_A = \frac{D_T \Delta T^*}{D_B T_u^* \left(\phi_u^* - \phi_l^*\right)}$, the increasing in D_T indicates instability in the temperature difference within the nanofluids layer. Therefore, as N_A increases, the thermal instability also increase and destabilizes the system.

Two important types of interdiffusion in this problem; Soret Sr and Dufour Df parameters are discussed briefly (Figures 7 and 8). The visual representation of Ra versus a shows the obtained results for both effects under lower free-upper free, lower rigid-upper free, and both rigid boundaries. Figure 7 depicts plots of Ra versus a for $Sr = 0.2, 0.4$, and 0.6. Ra clearly decreases as the parameter Sr increases, thus increasing the rate of convection in the system due to the increase in the temperature heat flux. The effect of the Dufour parameter ($Df = 0.2, 0.4$, and 0.6, Figure 8) on the system is opposite to that of the Soret parameter Sr. Increasing Df stabilizes the system because the Dufour energy flux increase the solute concentration by driving the mass gradient within the system, thus delaying the Rayleigh-Bénard convection. Therefore, both Soret and Dufour interdiffusion play important roles in the stability of this system.

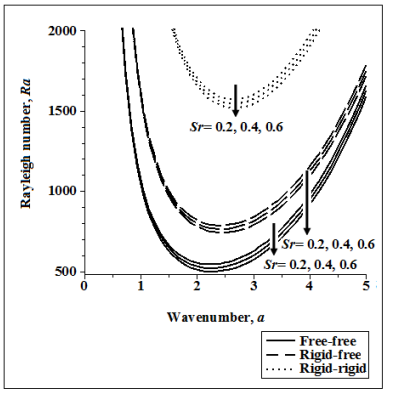

Figure 7: Ra against a for selected values of Sr.

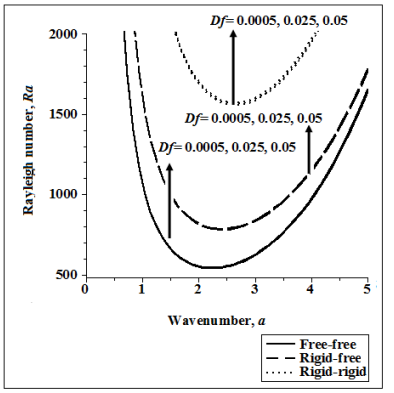

Figure 8: Ra against a for selected values of Df.

The presence of internal heat generation, $Q = 3, 9$ and Soret parameter, $Sr = 0.2, 0.6$ to the system for different values of magnetic field, H are plotted in Figures 9 and 10. Both figures show that the effect of magnetic field H slightly increases the values of critical Rayleigh number, Ra_c for internal heat generation Q and Soret parameter Sr. As expected the existence of magnetic field H has a positive significant effect to stabilise the nanofluid layer in the presence of internal heat generation Q and Soret parameter Sr.

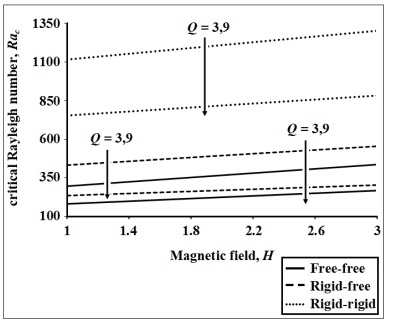

Figure 9: Ra_c against H for selected values of Q.

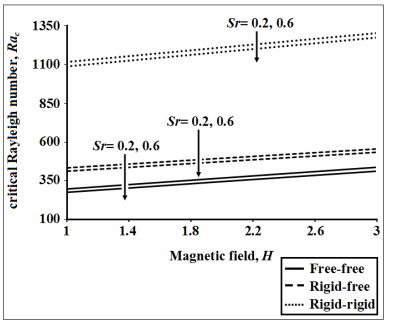

Figure 10: Ra_c versus H for selected values of Sr.

The influence of Dufour parameter, Df and solutal Rayleigh number, Rs to the Soret parameter, Sr are shown in Figures 11 and 12 respectively. In the respective figures, we observed that the critical Rayleigh number, Ra_c for the different values of Dufour parameter, $Df = 0.0005, 0.05$ and solutal Rayleigh number, $Rs = 100, 300$ decreases with the increase values of Soret parameter, Sr. Therefore, this observation shows that the increasing values of Soret parameter advancing in the onset of convection in a nanofluid system.

Figure 13 shows the plot of critical Rayleigh number, Ra_c for various values of internal heat generation, $Q = 3, 9$ against the Dufour parameter, Df. Clearly, the effect of internal heat generation, Q is known to hasten the onset of convection, but the process can be slowed down by adding the effect of Dufour parameter, Df.

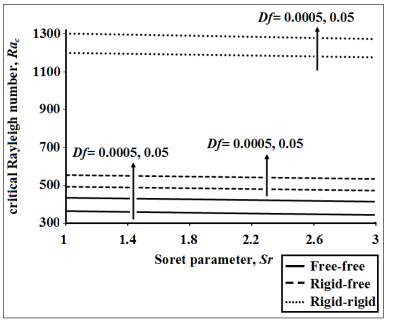

Figure 11: Ra_c versus Sr for selected values of Df.

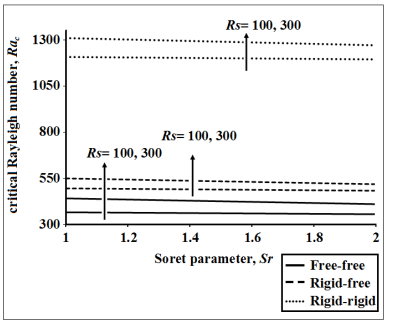

Figure 12: Ra_c versus Sr for selected values of Rs.

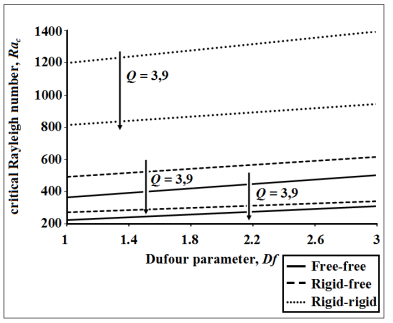

Figure 13: Ra_c versus Df for selected values of Q.

The interaction between the effect of nanofluid Rayleigh number, Rn on the critical Rayleigh number, Ra_c with solutal Rayleigh number, Rs can be seen in Figure 14. In the respective figure, it is observed that the presence of nanofluid Rayleigh number, Rn has a destabilizing effect where the increased values of nanofluid Rayleigh number, $Rn = 1, 3$ decreased the critical Rayleigh number, Ra_c. But by adding the effect of solutal Rayleigh number, Rs the process of heat transfer can be delayed.

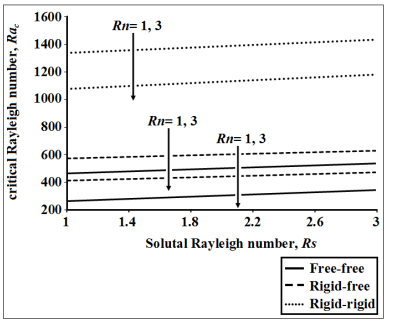

Figure 14: Ra_c versus Rs for selected values of Rn.

For all types of the lower-upper of free-free, rigid-free, and rigid-rigid boundaries, the rigid-rigid curves dominate the upper space of the graph in all of the respective figures. Obviously, the system is found to be more stable with rigid–rigid boundaries than with free-free and rigid-free boundaries.

4. Conclusions

The onset of double-diffusive magnetoconvection in nanofluids layer with internal heat generation in the presence of Soret and Dufour effects has been investigated analytically using linear stability theory. Three types of lower-upper boundaries of nanofluids layer are considered for free-free, rigid-free and rigid-rigid. The employed model for nanofluids combines the Brownian motion and thermophoresis mechanism. Buongiorno (2006) stated that these mechanisms were identified as the fundamental mechanism to advance the heat transfer in nanofluids layer system. The lower–upper bounding surfaces of the model system have been considered for free–free, rigid–free and rigid–rigid respectively. Linear stability analysis is used where the eigenvalue equation of the perturbed state is obtained from a normal mode analysis. Then, the eigenvalue equation is solved by applying the Galerkin method and computed numerically through Maple software. The results can be summarized as below:

1. The implementation of the effects of magnetic field, H, Dufour parameter Df and solutal Rayleigh number Rs is found to produce a lag on Rayleigh–Bénard convection in nanofluids layer system when the values of these parameters are increased thus stabilized the system.

2. The opposite outcome can be seen in the implementation effects of internal heat generation, Q, nanoparticles concentration Rayleigh number Rn and modified diffusivity ratio N_A advances the onset of Rayleigh–Bénard convection in nanofluids layer system when the values of these parameters are increased thus destabilized the system.

3. Based on the obtained results, the system of lower–upper free–free, rigid–free and rigid–rigid boundary conditions are found to be the most effectively stable with rigid–rigid boundaries whereas free–free is found to be the most unstable boundaries in the system.

Acknowledgment

The authors would like to thank the Ministry of Higher Education, Malaysia (MOHE) for FRGS Vote No 5524808 and UPM Vote No 9428400.

References

Agarwal, S., Bhadauria, B. S., Sacheti, N. C., Chandran, P., and Singh, A. K. (2012). Nonlinear convective transport in a binary nanofluid saturated porous layer. *Transport in Porous Media*, **93**(1):29–49.

Akbar, N., Khan, Z., Nadeem, S., and Khan, W. (2016). Double-diffusive natural convective boundary layer flow of a nanofluid over a stretching sheet with magnetic field. *International Journal of Numerical Methods for Heat and Fluid Flow*, **26**(1):108–121.

Bergeon, A., Henry, D., Benhadid, H., and Tuckerman, L. S. (1998). Marangoni convection in binary mixtures with soret effect. *Journal of Fluid Mechanics*, **375**:143–177.

Bhadauria, B. S., Kumar, A., Kumar, J., Sacheti, N. C., and Chandran, P. (2011). Natural convection in a rotating anistropic porous layer with internal heat generation. *Transport in Porous Media*, **90**:687–705.

Buongiorno, J. (2006). Convective transport in nanofluids. *ASME Journal of Heat Transfer*, **128**:240–250.

Caldwell, D. R. (1970). Non-linear effects in a rayleigh-benard experiment. *Journal of Fluid Mechanics*, **42**(1):161–175.

Capone, F., Gentile, M., and Hill, A. A. (2011). Double-diffusive penetrative convection simulated via internal heating in an anistropic porous layer with throughflow. *International Journal of Heat and Mass Transfer*, **54**:1622–1626.

Chand, R. and Rana, G. C. (2015). Magneto convection in a layer of nanofluid with soret effect. *Acta Mechanica et Automatica*, **9**(2):63–69.

Chandrasekhar, S. (1961). *Hydrodynamic and hydromagnetic stability*. Oxford University Press, UK, 1th edition.

Char, M. I. and Chiang, K. T. (1994). Stability analysis of benard-marangoni convection in fluids with internal heat generation. *Journal of Physics D: Applied Physics*, **27**:748–755.

Choi, S. U. S. (1995). *Developments and Applications of non-Newtonian Flows*. D. A. Siginer, H. P. Wang (Eds.), ASME FED 321/ MD, New York.

Friedrich, R. and Rudraiah, N. (1984). Marangoni convection in a rotating fluid layer with nonuniform temperature gradient. *International Journal of Heat and Mass Transfer*, **27**:443–449.

Gupta, U., Ahuja, J., and Wanchoo, R. K. (2013). Magneto convection in a nanofluid layer. *International Journal of Heat and Mass Transfer*, **64**:1163–1171.

Haddad, Z., Abu-Nada, E., Oztop, H. F., and Mataoui, A. (2012). Natural convection in nanofluids: Are the thermophoresis and brownian motion effects significant in nanofluids heat transfer enhancement? *International Journal of Thermal Sciences*, **57**:152–162.

Hurle, D. T. J. and Jakeman, E. (1971). Soret driven thermosolutal convection. *Journal of Fluid Mechanics*, **47**(4):668–687.

Khalid, I. K., Mokhtar, N. F. M., and Arifin, N. M. (2013). Uniform solution on the combined effect of magnetic field and internal heat generation on rayleigh-benard convection in micropolar fluid. *ASME Journal of Heat Transfer*, **135**:1–6.

Khalid, I. K., Mokhtar, N. F. M., Hashim, I., Ibrahim, Z. B., and Gani, S. S. A. (2017). Effect of internal heat source on the onset of double-diffusive convection in a rotating nanofluid layer with feedback control strategy. *Advances in Mathematical Physics*, :1–12.

Kim, J., Kang, Y. T., and Choi, C. K. (2004). Analysis of convective instability and heat transfer characteristics of nanofluids. *Physics of Fluids*, **16**(7):2395–2401.

Knobloch, E. and Moore, D. R. (1988). Linear stability of experimental soret convection. *Physics Review A*, **37**(3):860–870.

Kuznetsov, A. V. and Nield, D. A. (2010). The onset of double-diffusive nanofluid convection in a layer of a saturated porous medium. *Transport in Porous Media*, **85**(3):941–951.

Maekawa, T. and Tanasawa, I. (1988). Effect of magnetic field on onset of marangoni convection. *International Journal of Heat and Mass Transfer*, **31**(2):285–293.

Masuda, H., Ebata, A., Teramae, K., and Hishinuma, N. (1993). Alteration of thermal conductivity and viscosity of liquid by dispersing ultra-fine particles. *Netsu Bussei*, **7**:227–233.

Mokhtar, N. F. M., Arifin, N. M., Nazar, R., Ismail, F., and Suleiman, M. (2009). Marangoni convection in a liquid saturated porous medium with internal heat generation. *Far East Journal of Applied Mathematics*, **34**:269–283.

Mokhtar, N. F. M., Arifin, N. M., Nazar, R., Ismail, F., and Suleiman, M. (2010). Effect of internal heat generation on marangoni convection in a fluid saturated porous medium. *International Journal of Applied Mathematics and Statistics*, **19**:112–122.

Mokhtar, N. F. M., Arifin, N. M., Nazar, R., Ismail, F., and Suleiman, M. (2011). Effect of internal heat generation on marangoni convection in superposed fluid porous layer with deformable free surface. *International Journal of Physical Sciences*, **6**:5550–5563.

Mokhtar, N. F. M., Khalid, I. K., Siri, Z., Ibrahim, Z. B., and Gani, S. S. A. (2017). Control strategy on the double-diffusive convection in a nanofluid layer with internal heat generation. *Physics of Fluids*, **29**:1–10.

Nield, D. A. and Kuznetsov, A. V. (2010). The onset of convection in a horizontal nanofluid layer of finite depth. *European Journal of Mechanics-B/Fluids*, **29**(3):217–223.

Nield, D. A. and Kuznetsov, A. V. (2011). The onset of double-diffusive convection in a nanofluid layer. *Journal of Heat and Fluid Flow*, **32**(4):771–776.

Rama Rao, K. V. (1980). Thermal instability in a micropolar fluid layer subject to a magnetic field. *International Journal of Engineering Science*, **18**:741–750.

Rudraiah, N., Chandna, O. P., and Garg, M. R. (1984). Effect of nonuniform temperature gradient on magnetoconvection driven by surface tension and buoyancy. *Indian Journal of Technology*, **24**:279–284.

Saravanan, S. and Sivakumar, T. (2009). Exact solution of marangoni convection in a binary fluid with throughflow and soret effect. *Applied Mathematical Modelling*, **33**(9):3674–3681.

Slavtchev, S., Simeonov, G., Vaerenbergh, S. V., and Legros, J. C. (1999). Technical note marangoni instability of a layer of binary liquid in the presence of nonlinear soret effect. *International Journal of Heat and Mass Transfer*, **42**(15):3007–3011.

Tzou, D. Y. (2008a). Instability of nanofluids in natural convection. *ASME Journal of Heat Transfer*, **130**:372–401.

Tzou, D. Y. (2008b). Thermal instability of nanofluids in natural convection. *International Journal of Heat and Mass Transfer*, **51**:2967–2979.

Wilson, S. K. (1994). The effect of a uniform magnetic field on the onset of steady marangoni convection in a layer of conducting fluid with a prescribed heat flux at its lower boundary. *Physics of Fluids*, **6**:3591–3600.

Yadav, D., Agrawal, G. S., and Bhargava, R. (2011). Rayleigh-bénard convection in nanofluid. *International Journal of Applied Mathematics and Mechanics*, **7**:61–76.

Yadav, D., Agrawal, G. S., and Bhargava, R. (2012a). The onset of convection in a binary nanofluid saturated porous layer. *International Journal of Theoretical and Applied Multiscale Mechanics*, **2**(3):198–224.

Yadav, D., Agrawal, G. S., and Bhargava, R. (2012b). The onset of convection in a binary nanofluid saturated porous layer. *International Journal of Theoretical and Applied Multiscale Mechanics*, **2**(3):198–224.

Yadav, D., Agrawal, G. S., and Lee, J. (2016). Thermal instability in a rotating nanofluid layer: A revised model. *Ain Shams Engineering Journal*, **7**:431–440.

Yadav, D., Kim, C., Lee, J., and Cho, H. H. (2015). Influence of magnetic field on the onset of nanofluid convection induced by purely internal heating. *Computers and Fluids*, **121**:26–36.

Yadav, D., R. Bhargava, R., and Agrawal, G. S. (2013). Thermal instability in a nanofluid layer with a vertical magnetic field. *Journal of Engineering Mathematics*, **80**:147–164.